ARTICLE
Journal of Cellular Biochemistry 114:2101–2113 (2013)

Journal of Cellular Biochemistry

Gremlin Aggravates Hyperglycemia-Induced Podocyte Injury by a TGFβ/Smad Dependent Signaling Pathway

Guiying Li,[1,2] Ying Li,[1]* Shuxia Liu,[3] Yonghong Shi,[3] Yanqing Chi,[1] Guijing Liu,[2] and Tieying Shan[2]

[1]*Department of Nephrology, Third Hospital, Hebei Medical University, Shijiazhuang, 050051, China*
[2]*Department of Nephrology, Affiliated Hospital of Hebei Engineering University, Handan, 056029, China*
[3]*Department of Pathology, Hebei Medical University, Shijiazhuang, 050071, China*

ABSTRACT

Gremlin is a bone morphogenic protein (BMP) antagonist and is elevated in diabetic kidney tissues. In the early course of diabetic nephropathy (DN), podocyte are injured. We studied the protein and gene expression of gremlin in mice podocytes cultured in hyperglycemia ambient. The role of gremlin on podocyte injury and the likely signaling pathways involved were determined. Expression of gremlin was visualized by confocal microscopy. Recombinant mouse gremlin and small interfering RNA (siRNA) targeting to gremlin1 identified the role played by gremlin on podocytes. Study of canonical (smad2/3) and non-canonical (p38MAPK and JNK1/2) transforming growth factor beta (TGFβ)/smad mediated signaling revealed the putative signaling mechanisms involved. Smad2/3 siRNA and TGFβ receptor inhibition (SB431542) were used to probe canonical TGFβ/smad signaling in gremlin-induced podocyte injury. Apoptosis of podocytes was measured by TUNEL assay. Gremlin expression was enhanced in high glucose cultured mouse podocytes, and was localized predominantly in the cytoplasm and negligibly on the cell membrane. Not only expression of nephrin and synaptopodin were decreased on treatment with gremlin, but also synaptopodin rearrangement and nephrin relocalization were evident. Knockdown gremlin1 or smad2/3 by siRNA, and inhibition of TGFβR (SB431542) attenuated podocyte injury. Inhibition of canonical TGF-β signal blocked the injury of gremlin on podocytes. In conclusion, gremlin was clearly elevated in high glucose cultured mouse podocytes, and likely employed endogenous canonical TGFβ1/Smad signaling to induce podocyte injury. Knockdown gremlin1 by siRNA may be clinically useful in the attenuation of podocyte injury. J. Cell. Biochem. 114: 2101–2113, 2013.

KEY WORDS: GREMLIN1; INJURY, MOUSE PODOCYTE; SMAD; TRANSFORMING GROWTH FACTOR BETA1

Gremlin is a developmental gene and is associated with dibetic nephropathy (DN) [Lappin et al., 2000]. It contains potential nuclear localization sites near its carboxyl-terminus, N-linked glycosylation sites, and a number of phosphorylation sites [Wada et al., 2011]. Gremlin is also a 23–28 kDa secreted protein, which is present as both soluble and cell-associated forms and is found within the Golgi apparatus and endoplasmic reticulum [Smerdel-Ramoya et al., 2011]. Bone morphogenic protein (BMP)-2, BMP-4, and BMP-7 are directly bound to, or heterodimerized by gremlin, and as a consequence, lose their ability to bind to their receptors and to exert a renoprotective effect [Murphy et al., 2002].

Expression of gremlin is found in the diabetic nephropathy kidney but not in the normal kidney [Dolan et al., 2003]. Using suppression-subtractive hybridization, gremlin1 was cloned and characterized, and was found to be upregulated in primary human renal mesangial cells cultured with high glucose (30 mmol/L) [Murphy et al., 2008]. IHG-2 is the human homolog of murine gremlin, which is also over expressed in renal biopsy specimens taken from human subjects presenting with diabetic nephropathy [McMahon et al., 2000]. Kidney mesangial and tubular cells exposed to high extracellular glucose were found to express high levels of gremlin [Dolan et al., 2005; Zhang et al., 2010]. In addition, it has been found that TGF-β can

Conflict of interest: none.

* Correspondence to: Ying Li, Department of Nephrology, Third Hospital, Hebei Medical University, Shijiazhuang 050051, China. E-mail: fflgy@126.com

Manuscript Received: 4 january 2013; Manuscript Accepted: 18 March 2013
Accepted manuscript online in Wiley Online Library (wileyonlinelibrary.com): 1 April 2013
DOI 10.1002/jcb.24559 • © 2013 Wiley Periodicals, Inc.

induce transcriptional and protein expression of gremlin [Dolan et al., 2003] and that gremlin can reversibly induce the expression of TGF-β2 in trabecular meshwork cells [Sethi et al., 2011].

However, few studies have assessed the regulation of gremlin expression under conditions of culturing podocytes in high glucose. It was previously shown that the podocyte was injured in the early course of DN, and that this phase of podocyte injury preceded the changes seen in the GBM and mesangial area by several years [Jefferson et al., 2011]. The role of the glomerular podocyte in the progression of DN is of increasing interest [Diez-Sampedro et al., 2011]. An early and key event in the development of DN is high-motility and loss of podocytes from the kidney glomerulus [Babayeva et al., 2011]. The mechanism remains poorly defined. Thus, the objective of the present study was to determine the functional expression of gremlin and its effect on podocytes cultured in high glucose. Additionally, we wished to gain insights into the likely signaling pathway that were involved in gremlin-mediated podocytes injury.

MATERIALS AND METHODS

CELL CULTURE

Experiments were performed using a thermosensitive SV-40-transfected immortalized mouse podocyte cell-line (H-2K^b-tsA58, 3111c0001ccc000230, National Cell Resource Center of China, Beijing). Podocytes were cultured in Dulbecco's modified Eagle's medium (DMEM) supplemented with 100 U/ml penicillin, 100 μg/ml streptomycin and 10% fetal bovine serum (FBS). Cells were grown at 33°C (permissive conditions) and treated with mouse recombinant γ-interferon at 10 U/ml (Sigma, St. Louis, MO). When cells had obtained a confluence of 80%, podocytes were cultured at 37°C (non-permissive conditions) without IFN-γ for 10–14 days to induce differentiation. Podocytes could then be used in the next stage of the study.

CELL TREATMENT

Podocytes (37°C) were grown to 80% confluence and retained in serum-free culture medium for 24 h before treatment so that the effects of serum proteins did not influence cellular behavior, then incubated with fresh culture medium containing D-glucose at a normal concentration of 5.5 mmol/L, or at a high D-glucose concentration of 30 mmol/L. In addition, cells were cultured in medium containing 5.5 mmol/L D-glucose plus 19.5 mmol/L D-mannitol to control the osmotic effects of a high glucose concentration. In dose-ranging studies, recombinant gremlin protein (R&D System, Minneapolis, MN) was incubated with the podocytes exposed to high D-glucose for 48 h so that the optimal concentration could be determined. The small molecule inhibitor SB431542 (Sigma–Aldrich) was used at a concentration of 5 μM to study the effects of inhibiting the TGF-β receptor 1/2. The expression levels of smad2/3, JNK1/2, and p38MAPK were determined to find the likely signaling pathway that was mechanistically involved in the response of podocytes to gremlin. Smad2/3 and gremlin1 specific siRNA was used to study the effects of inhibiting canonical smad signaling pathways and the protective effects of knocking down the expression of gremlin1. All experiments were done in triplicate. Cells were harvested for total RNA, protein extraction and for other experiments described below.

SMALL INTERFERING RNA AND TRANSFECTION

siRNAs targeting against smad2/3(sc-37239) and gremlin1(sc-39409) were obtained from Santa Cruz Inc. (San Diego, CA). siRNA transfection was performed in accordance with the manufacturer's instructions. Briefly, podocytes were seeded at a density of 2×10^5 per well in 6-well plates containing antibiotic-free normal culture medium that was supplemented with 10% FBS and incubated for 24 h at 37°C in a fully-humidified 5% CO_2 incubator, then serum-starved for 24 h immediately afterwards. In one tube, 6 μl of siRNA transfection reagent (sc-29528) was mixed gently with 100 μl siRNA transfection medium (sc-36868). In separate tubes, siRNA duplex (60–80 pmols) was mixed gently with 100 μl of transfection medium. The siRNA duplex solution was added directly to the diluted transfection reagent using a pipette, mixed gently up and down, and the mixture incubated for 30 min at room temperature. siRNA transfection medium (0.8 ml) was added to each mixture. The cells were washed once with 2 ml of siRNA transfection medium, incubated with the siRNA transfection solution for 6 h at 37°C in a fully-humidified 5% CO_2 incubator, washed with normal medium, then incubated with DMEM containing 10% FBS for 24 h. They were then washed with serum-free DMEM and treated with medium containing high D-glucose or gremlin for an additional 48 h. All experiments were carried out in triplicate. Cells were harvested for total RNA, protein extraction, and for other experiments as described below.

RNA ISOLATION AND QUANTITATIVE REAL-TIME PCR

Total RNA was extracted using TRIzol Reagent™ (Invitrogen, Carlsbad, CA) according to the manufacturer's instructions. The RNA concentration and purity was assessed by UV spectroscopy. Structural integrity of the RNA samples was confirmed by electrophoresis using 1% (w/v) agarose gels. Total cellular RNA was converted to cDNA using a cDNA synthesis kit (primescript® RT reagent kit, Takara). Primers for the various genes were designed using the primer bank for real-time PCR. The primer pairs are listed in Table I. A real-time PCR kit (SYBR® premix Ex Taq™, Takara) was used to quantitatively evaluate target gene expression. Briefly, 2 μl of cDNA was used in a reaction mixture consisting of 12.5 μl SYBR® premix Ex Taq enzyme, 0.5 μl ROX reference II, 100 nmol PCR primers (Table I) as well as sterile dH_2O to a total volume 25 μl per reaction. PCR was performed on a real-time thermal cycler (model Mx3005p; Stratagene, USA), with cycling parameters of an initial denaturation at 95°C for 5 min; 40 cycles of 95°C for 30 s, 60°C for 30 sec, and 72°C for 60 s, and a denaturation cycle for the creation of dissociation curves. Reactions for each sample were run in duplicate, cycle thresholds (C_t) were normalized to GAPDH expression as the housekeeping gene, and comparative quantitation was performed (MxPro ver 4.1 software; Stratagene). Only individual PCR samples with single-peak dissociation curves were selected for data analysis. RNA that was not reverse transcribed served as a negative control.

PROTEIN EXTRACTION AND WESTERN IMMUNOBLOT ANALYSIS

Total protein was extracted from the podocytes using a mammalian protein extraction buffer, containing protease and phosphatase

TABLE I. Primers Used for Real-Time PCR Studies

Gene	Primers (5′ → 3′)	Products size (bp)
GREM1		
Forward	AAGCGAGACTGGTGCAAAAC	158
Reverse	CTTGCAGAAGGAGCAGGACT	
TGF-β1		
Forward	ACCGCAACAACGCAATCTATG	196
Reverse	ATTCCGTCTCCTTGGTTCAG	
NEPHRIN		
Forward	TACCACCAGCATTTCCACG	185
Reverse	GGGCTCGGCTGTATGTATT	
SYNAPTOPODIN		
Forward	ACTTCCGTGGAGCTGCTTTC	186
Reverse	CCCGAGGACAGATGTTGTAG	
BCL-2		
Forward	ATGCCTTTGTGGAACTATATGGC	120
Reverse	GGTATGCACCCAGAGTGATGC	
BAX		
Forward	AGACAGGGGCCTTTTTGCTAC	137
Reverse	AATTCGCCGGAGACACTCG	
CASEPASE-3		
Forward	CACTGGAATGTCAGCTCGCA	156
Reverse	TCAGGGCCATGAATGTCTCTC	
GAPDH		
Forward	CCCACTAACATCAAATGGGG	198
Reverse	ATCCACAGTCTTCTGGGTGG	

inhibitor cocktails. The total protein concentration was determined by the BCA protein assay (BCA, China). The cellular proteins were separated on 10–12% denaturing polyacrylamide gels and then transferred to PVDF membranes by electrophoresis. Blots were blocked in 5% fat-free dry milk proteins in TBST for 2 h and incubated overnight with primary antibodies (Table II). The membranes were washed in TBST and incubated with the corresponding horseradish peroxidase (HRP)-conjugated secondary antibodies. The proteins were then visualized (Oddsay, USA) using ECL detection reagent (Tiangen, 102191, China). To ensure equal protein loading, the same blot was subsequently re-probed and developed for β-actin expression.

IMMUNOSTAINING

The immunolabeling was done as previously described [Faul et al., 2008]. Briefly, coverslips were fixed in 4% paraformaldehyde in phosphate-buffered saline (PBS) for 30 min, then permeabilized with 0.3% Triton X-100 (Sigma) in PBS for 10 min. Non-specific binding sites were blocked with 4% FBS and 0.1% Tween 20 (Sigma) in PBS for 30 min. The coverslips were incubated with anti-synaptopodin or anti-nephrin at 4°C overnight in a wet box. Next, FITC-conjugated secondary antibodies were applied at the appropriate dilutions and according to standard techniques. The coverslips were washed several times (while avoiding direct sunlight) and mounted on glass slides with 15% Mowiol (Calbiochem, La Jolla, CA, USA) and 50% glycerol in PBS. Images were obtained by confocal laser-scanning microscopy using a Leica TCS NT confocal system attached to a Leica DM RBE microscope and equipped with an ArKr laser (488 nm excitation, Leica Microsystems, Heidelberg, Germany). An oil-immersion objective lens with a numerical aperture of 1.32 was used and imaging parameters selected to optimize confocal resolution. To control for non-specific binding of secondary antibodies, negative controls were performed, which were handled similarly, but incubated in PBS/BSA.

APOPTOSIS ASSAY

Apoptotic nuclei were detected by a transferase-mediated dUTP nick-end labeling (TUNEL) assay of podocytes. The TUNEL assay was used according to the manufacturer's protocol (Promega Inc, USA). Nuclear staining was also used to assess apoptosis by staining

TABLE II. List of Various Antibodies Used for Western Immunoblot Studies

Antibody	Dilution	Source
Rabbit anti-gremlin1	1:200	Sant Cruz
Rabbit anti-TGFβ1	1:500	Proteintech
Rabbit anti-nephrin	1:100	Bionson
Rabbit anti-synaptopodin	1:1,000	Abcam
Rabbit anti-smad2/3	1:500	Bioss
Rabbit anti-phos-smad2	1:500	Bioss
Rabbit anti-phos-smad3	1:500	Bioss
Rabbit anti-JNK1/2	1:500	Cell Signaling
Rabbit anti-phos-JNK1/2	1:500	Cell Signaling
Rabbit anti-p38	1:1,000	Cell Signaling
Rabbit anti-phos-p38	1:1,000	Cell Signaling
Rabbit anti-Bcl-2	1:500	Bioss
Rabbit anti-Bax	1:500	Bioss
Rabbit anti-caspase-3	1:500	Bioss
Goat anti-rabbit IgG	1:10,000	Bioss

podocytes with propidium iodide (PI). Apoptotic nuclei were observed as small, condensed, symmetrical spheres that were located adjacent to the nucleus. For quantification of TUNEL-positive (apoptotic) cells, a minimum of 200 cells were counted per group, and the percentage of the positively labeled cells was calculated. To further assess the apoptosis and reduce the influence of necrosis, the expression of Bcl-2, Bax and Cleaved Caspase-3 were assayed at protein and mRNA level in each group.

STATISTICAL ANALYSIS

All values are reported as mean ± standard deviation (SD) about the mean. One-way analysis of variance (ANOVA) was used for comparison of the results between more than two groups. Statistical significance was defined as an alpha value of $P < 0.05$. The statistical analyses were carried out using the SAS statistical software (ver. 8.1, Cary, NC).

RESULTS

GREMLIN1 WAS OVER-EXPRESSED IN HIGH D-Glucose Ambient Podocytes

Gremlin1 was elevated significantly in high-glucose cultured murine podocytes both at the protein and mRNA levels (0.81 ± 0.012, 0.66 ± 0.015), but seldom in normal glucose (0.38 ± 0.039, 0.031 ± 0.012) or mannitol controls (0.35 ± 0.015, 0.29 ± 0.013; Fig. 1A–C). Confocal staining demonstrated that the distribution of gremlin1 in podocytes was located predominantly in the cytoplasm, sparsely on the cell membrane and was associated with a punctate pattern (Fig. 1D).

GREMLIN AGGRAVATED HIGH-GLUCOSE CULTURED PODOCYTE INJURY

Gremlin, at a dose of 0.75 μg/ml for 48 h in high glucose medium, down-regulated the transcriptional and protein expression of both synaptopodin and nephrin (Fig. 2A). The distribution of nephrin differed markedly between podocytes cultured in the presence of gremlin and control cells. Control cells expressed nephrin in cell projectons or exhibited a filamentous nephrin appearance. By contrast, cells cultured with gremlin displayed a cytoplastic and non-filamentous distribution (Fig. 2A). In gremlin-cultured podocytes, synaptopodin distributed mainly at peri- or intra-nuclear regions (Fig. 2A). In normal control cells, synaptopodin localized mainly in the foot process or cytoplasm in a punctuated pattern along actin filaments. High-glucose induced synaptopodin shifting to the cytoplasm and depolymerization of actin mirofilaments. Gremlin aggravated such injury and induced a marked decrease in podocyte

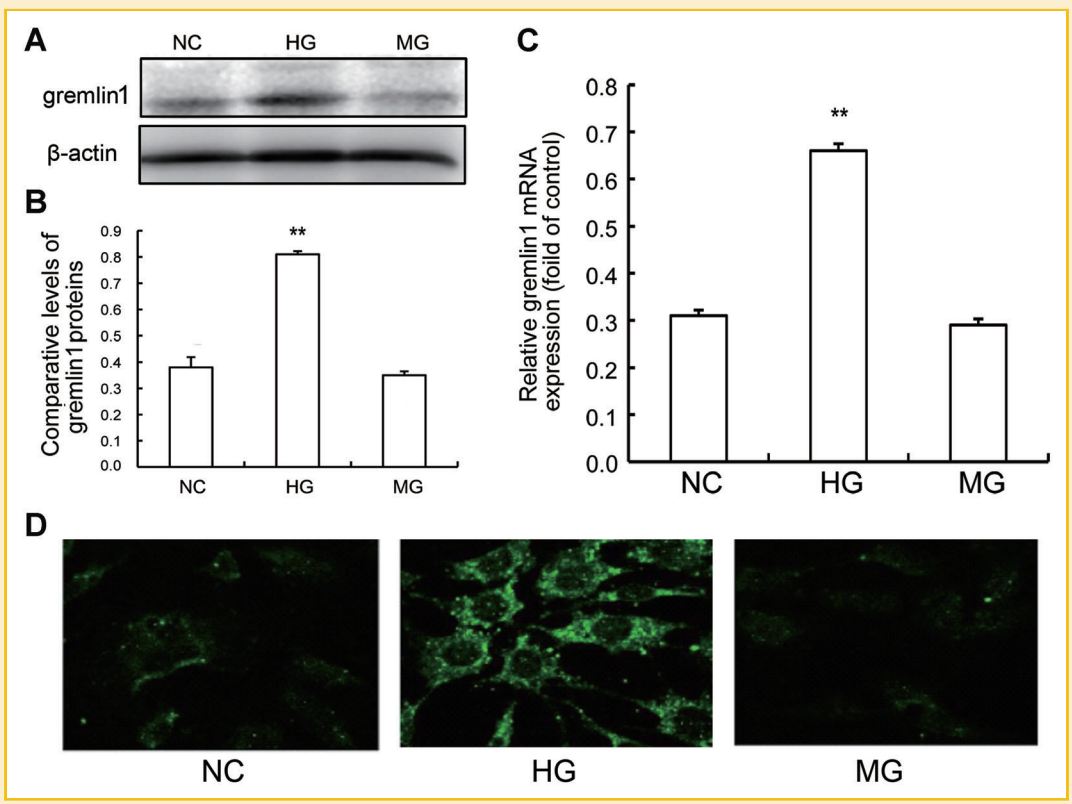

Fig. 1. The expression and distribution of gremlin in ambient high glucose podocytes for 48 h. A: Gremlin protein was analyzed by Western immunoblot. B: The gremlin protein was quantified by densitometry. β-actin was used as the loading control. C: qRT-PCR values represented the ratio of gremlin normalized to GAPDH in treated samples and controls. D: Representative confocal images of gremlin protein. Gremlin expression was elevated significantly under hyperglycemic conditions, locating mainly in the cytoplasm and significantly less at the cell membrane in a punctuate pattern (at 600× magnification). NC, normal control, D-glucose 5.5 mmol/L; HG, high-glucose, D-glucose 30 mmol/L; MG, mannitol 19.5 mmol/L + D-glucose 5.5 mmol/L. Values are expressed as the mean ± SD. n = 6. $^{**}P < 0.01$ versus NC group.

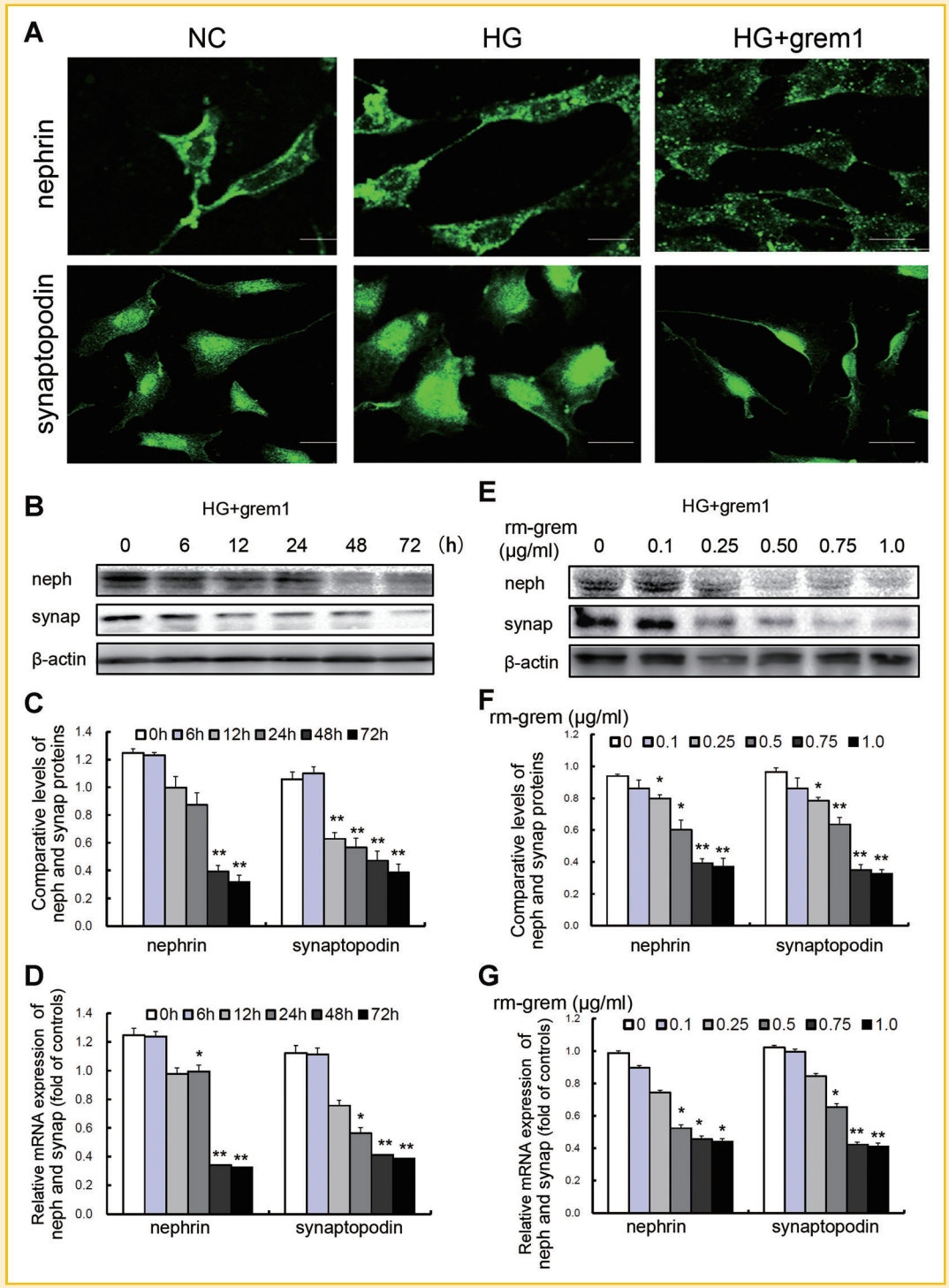

Fig. 2. Gremlin1 (0.75 μg/ml) aggravated hyperglycemia-induced podocyte injury. A: The representative confocal images of nephrin and synaptopodin. Gremlin1 down-regulated podocyte nephrin and synaptopodin expression and altered their distribution on incubation for 48 h. The up lane described nephrin. The low lane represented synaptopodin. B–D: Time-dependent (0–72 h) exposure of podocytes to gremlin (0.75 μg/ml) and high glucose (30 mmol/L) gradually decreased podocyte nephrin and synaptopodin protein (B,C) and mRNA (D) expression. E–G: Concentration-dependent (0–1 μg/ml) decreasement of nephrin and synaptopodin protein (E,F) and mRNA (G) expression on exposure of podocytes to gremlin in high glucose cultured podocytes. Western blots are representative data obtained from podocytes. The qPCR values represent induction of gremlin as compared with controls and normalized to GAPDH as the housekeeping gene. Three replicates of each sample were used. Values are expressed as the mean ± SD, n = 6. $^{*}P < 0.05$ and $^{**}P < 0.01$ versus controls (0 h or 0 μg/ml).

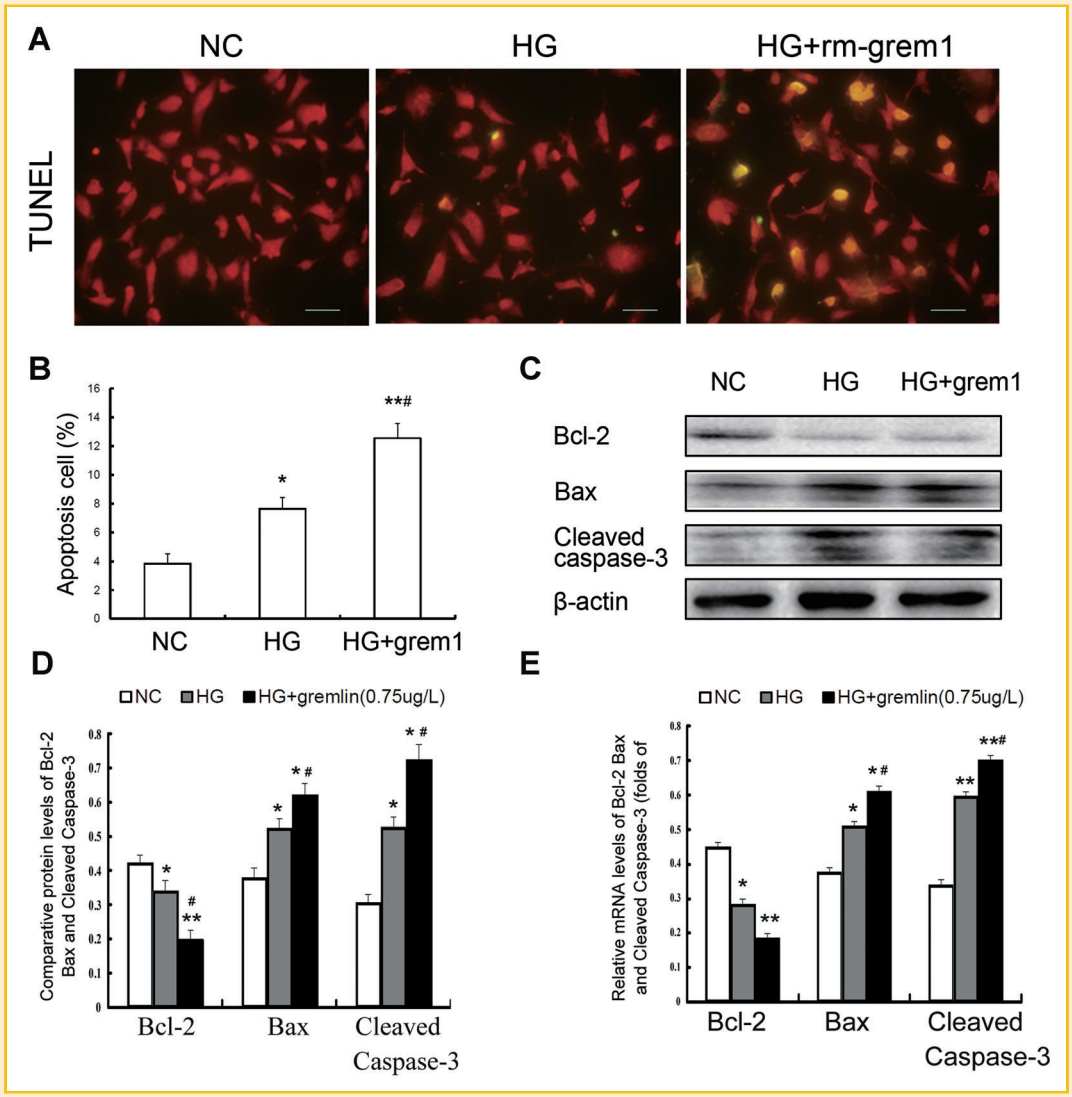

Fig. 3. Gremlin aggravated high glucose-induced podocyte apoptosis for 48 h. A: TUNEL staining showed green fluorescence of apoptosis cells (at 400× magnification). B: TUNEL-positive cell were counted out of a total of more than 200 cells over six random fields. The results were expressed as apoptosis cell (%). C: The protein expression of Bcl-2, Bax, and Cleaved Caspase-3 was analyzed by Western blot. D: The protein levels of Bcl-2, Bax, and Cleaved Caspase-3 was quantified by densitometry. E: The mRNA level of Bcl-2, Bax, and Cleaved Caspase-3 was analyzed by qRT-PCR. NC, normal control, D-glucose 5.5 mmol/L; HG, D-glucose 30 mmol/L; HG + grem, D-glucose 30 mmol/L + gremlin 0.75 μg/ml. The values were expressed as means ± SD, n = 6. $^{*}P < 0.05$, $^{**}P < 0.01$ versus NC group; $^{\#}P < 0.05$ versus HG group.

size, and rearrangement of synaptopodin from a linear and punctuated pattern to a granular mass.

Gremlin aggravated podocyte injury in a concentration- and time-dependent fashion. Podocytes were exposed to D-glucose (30 mmol/L) and gremlin1 (0.75 μg/ml) for different time periods (0, 6, 12, 24, 48, and 72 h). At 48 h, exposure of podocytes to gremlin1 promoted a maximal negative effect on the expression of nephrin and synaptopodin (Fig. 2B–D). Various concentrations of gremlin1 (0, 0.1, 0.25, 0.5, 0.75, and 1 μg/ml) were added to the culture medium concomitantly with D-glucose (30 mmol/L), and incubated with the podocytes for 48 h. At a dose of 0.75 μg/ml, gremlin1 maximally down-regulated the expression of both nephrin and synaptopodin (Fig. 2E–G).

Gremlin (0.75 μg/ml) was also found to exacerbate high-glucose induced podocyte apoptosis (Fig. 3A,B). Induction of podocyte apoptosis by gremlin was more common than in normal or hyperglycemic control cultures (12.562 ± 1.034%, 3.843 ± 0.678%, and 7.647 ± 0.769%, respectively). Apoptotic nuclei were detected as small, condensed, and symmetrical spheres that were located adjacently to the nucleus. On the other hand, Bcl-2, Bax, and Cleaved Caspase-3 are well recognized indicators of apoptosis, which are complementary with TUNEL in assessing apoptosis. As shown in Figure 3C,D, the results of Western blots indicated the protein levels of Bax and Cleaved Caspase-3 were markedly increased in HG + grem group when compared with HG or NC group. The qRT-PCR analysis also revealed that the mRNA level of Bcl-2 was decreased, but those of

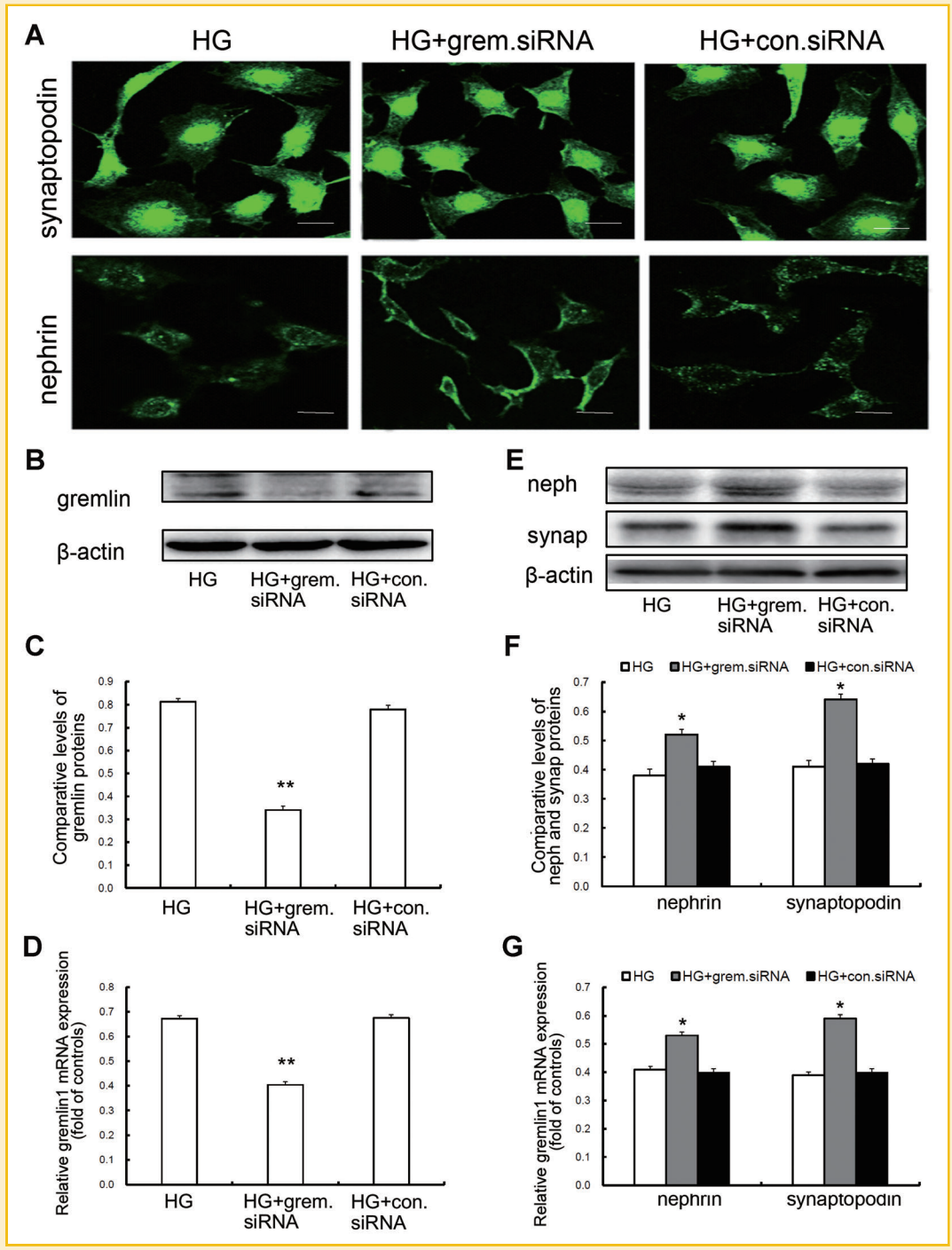

Fig. 4. Gremlin1 siRNA rescued the distribution and expression of nephrin and synaptopodin. A: Representative confocal images were displayed. B–D: Gremlin1 siRNA significantly knocked down the expression of gremlin1 at both the protein (B,C) and mRNA levels (D). E–G: Gremlin1 siRNA rescued the expression of nephrin and synaptopodin at both the protein (E,F) and mRNA (G) levels in high glucose treated podocytes. Western blots were representative of data obtained from cultured podocytes. qRT-PCR values represent the ratio of gremlin to GAPDH. Three replicates of each sample were used. HG, D-glucose 30 mmol/L; HG + grem.siRNA, D-glucose 30 mmol/L + gremlin siRNA 80 pmol/well; HG + con.siRNA, D-glucose 30 mmol/L + scramble siRNA 80 pmol/well. The values were expressed as means ± SD, n = 6. $^{*}P < 0.05$, $^{**}P < 0.01$ versus HG group.

Bax and Cleaved caspase-3 were increased significantly in HG + grem group (Fig. 3E).

siRNA TARGETING OF GREMLIN1 ATTENUATES INJURY OF PODOCYTES CULTURED IN HIGH GLUCOSE

Podocytes were cultured in ambient hyperglycemic conditions and transfected with Gremlin1 siRNA (80 pmol/well) to enforce down-regulation in the protein expression and mRNA expression of gremlin1. As shown in Figure 4, confocal images show that gremlin1 siRNA attenuated the distribution of nephrin and synaptopodin as compared to that of cells cultured in high glucose (Fig. 4A). Gremlin1 siRNA attenuated the distribution of nephrin from the cytoplasm and non-filamental to the cell membrane and filament pattern, and that of synaptopodin from granular to punctate and filamental pattern. The expression of gremlin protein (Fig. 4B,C) and mRNA (Fig. 4D) was knockdown markedly. Western immunoblot and real-time PCR analysis indicated that gremlin1 siRNA rescued the expression of nephrin and synaptopodin at both the protein and mRNA levels (Fig. 4E–G).

Gremlin siRNA decrease the percentage of TUNEL-positive cells. As shown in Figure 5A and B, there were 7.021% apoptosis cells in HG group and 4.986% apoptosis cells in HG+ grem.siRNA group. The

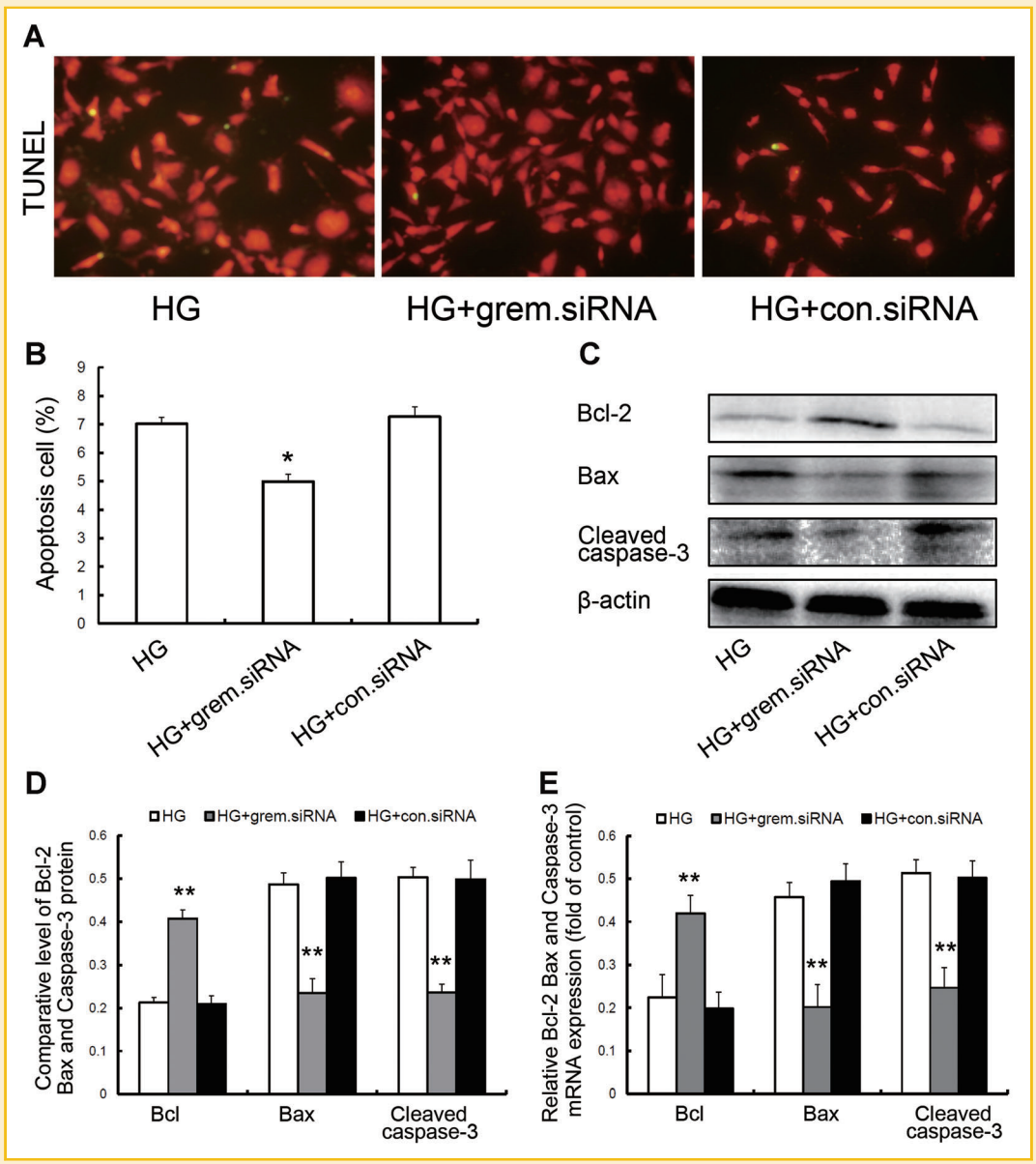

Fig. 5. Gremlin siRNA attenuated high glucose-induced podocyte apoptosis for 48 h. A: TUNEL staining showed green fluorescence of apoptosis cells (at 400× magnification). B: TUNEL-positive cell were counted out of a total of more than 200 cells over six random fields. The results were expressed as apoptosis cell (%). C: The protein expression of Bcl-2, Bax, and Cleaved Caspase-3 was analyzed by Western blot. D: The protein levels of Bcl-2, Bax and Cleaved Caspase-3 was quantified by densitometry. E: The mRNA level of Bcl-2, Bax and Cleaved Caspase-3 was analyzed by qRT-PCR. HG, D-glucose 30 mmol/L; HG + grem.siRNA, D-glucose 30 mmol/L + gremlin siRNA 80 pmol/well; HG + con.siRNA, D-glucose 30 mmol/L + scramble siRNA 80 pmol/well. The values were expressed as means ± SD, n = 6, $^{*}P < 0.05$ versus HG group.

scramble siRNA had no influence on apoptosis in high glucose conditions. Gremlin siRNA increase the expression of Bcl-2 and decrease that of Bax and Cleaved Caspase-3 in HG ambient (Fig. 5C–E). Gremlin siRNA attenuated effectively HG induced apoptosis.

TGF-β1 AND GREMLIN INDUCED EACH OTHER

Podocytes that were cultured in gremlin1 (0.75 μg/ml) concomitant with high glucose (30 mmol/L) for 48 h expressed TGF-β1 more abundantly than high glucose and normal controls at both the protein (1.21 ± 0.025, 0.92 ± 0.031 vs. 0.67 ± 0.021) and mRNA (1.13 ± 0.012, 0.89 ± 0.013 vs. 0.62 ± 0.012) levels. Conversely, podocytes that were cultured in TGF-β1 (5 ng/ml) concomitantly with high glucose (30 mmol/L) for 48 h expressed gremlin1 more abundantly than high glucose and normal controls at both the protein (0.85 ± 0.030, 0.64 ± 0.029 vs. 0.32 ± 0.024) and mRNA (0.79 ± 0.012, 0.62 ± 0.012 vs. 0.35 ± 0.011) levels (Fig. 6A–C).

ROLE OF TGF-β SIGNALING IN GREMLIN-MEDIATED PODOCYTE INJURY

TGF-β not only plays an important role in diabetic nephropathy, but it also has a close connection with bone morphogenetic protein (BMP), the molecule associated with the TGF-β signaling pathway. TGF-β pathway associated molecules were assayed in gremlin1 and high-glucose cultured podocytes (Fig. 7). Podocytes were treated with 0.75 μg/ml recombinant mouse gremlin and D-glucose (30 mmol/L) for various times (0, 15, 30, 60, 120, and 240 min, respectively), following which total protein (Fig. 7A) and total mRNA (Fig. 7B) was extracted to determine the expression of the canonical smad (smad2/3) and non-canonical JNK1/2 and p38MAPK signaling molecules. Untreated and inhibitor-treated cells served as negative controls. In gremlin-activated podocytes, smad2 and smad3 were phosphorylated in a time-dependent manner. By contrast, neither JNK1/2 nor p38MAPK were activated. Gremlin activated canonical, but not non-canonical signaling pathway in podocytes.

TGF-β receptor inhibitors (SB431542) blocked the ability of gremlin1 to suppress nephrin and synaptopodin expression (Fig. 7C,D). Podocytes were pretreated with SB431542 for 1 h, and then incubated with gremlin (0.75 μg/ml) and D-glucose (30 mmol/L) for an additional 48 h. Inhibition of the TGF-β receptor with SB431542 (5 μM/L) blocked the effect of gremlin1 on high glucose cultured podocytes and rescued the expression of nephrin and synaptopodin. Gremlin injured podocytes required endogenous expression of TGF-β.

Smad2/3 siRNA treatment inhibited the ability of gremlin to down-regulate the expression of nephrin and synaptopodin in high-glucose ambient podocytes. Podocytes were pretreated with smad2/3 siRNA (60 pmol/well) for 1 h before treatment with gremlin and high glucose. Control cells were transfected with scrambled siRNA sequences. Smad2/3 siRNA markedly knocked down its target protein and mRNA expression. Smad2/3 siRNA knockdown rescued the expression of both nephrin and synaptopodin and attenuated injury of podocytes that had been cultured in high glucose (Fig. 7E,F).

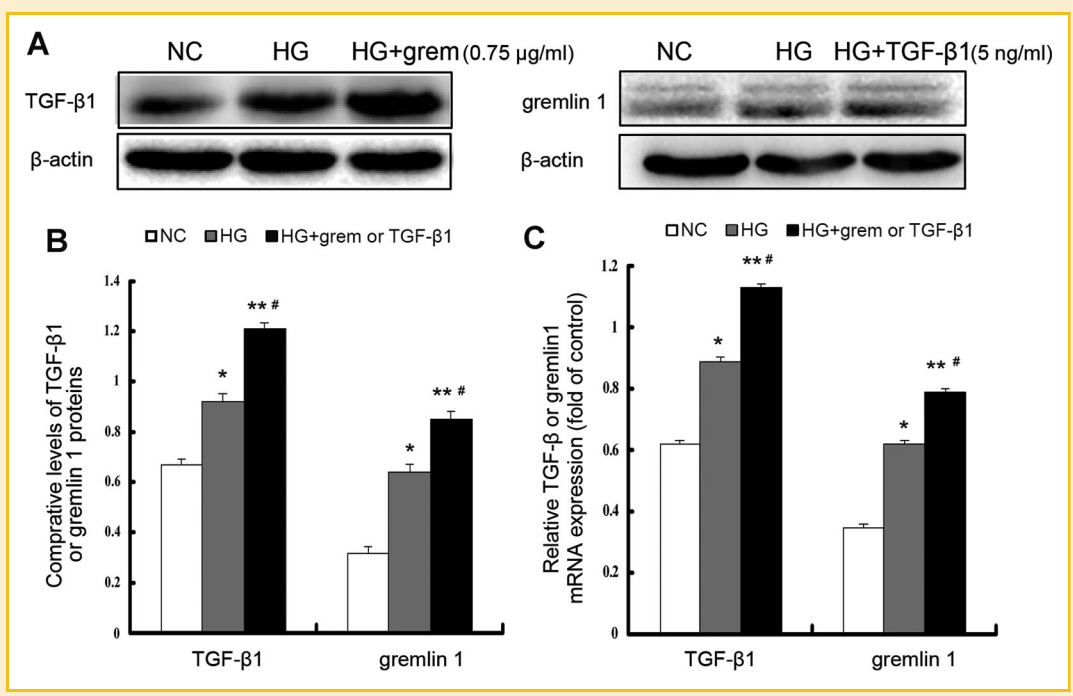

Fig. 6. TGF-β1 and gremlin induced each other's expression in high ambient glucose ambient. A: TGF-β1 or gremlin protein was analyzed by Western blot. B: The protein level of TGF-β1 or gremlin were quantified by densitometry. C: The mRNA expression of TGF-β1 or gremlin were quantified by qRT-PCR. NC, normal control, D-glucose 5.5 mmol/L; HG, D-glucose 30 mmol/L; HG + grem, D-glucose 30 mmol/L + gremlin 0.75 μg/ml; HG + TGF-β1, D-glucose 30 mmol/L + TGF-β1 5 ng/ml. The values were expressed as means ± SD, n = 6, $^{*}P < 0.05$; $^{**}P < 0.01$ versus NC group; $^{\#}P < 0.05$ versus HG group.

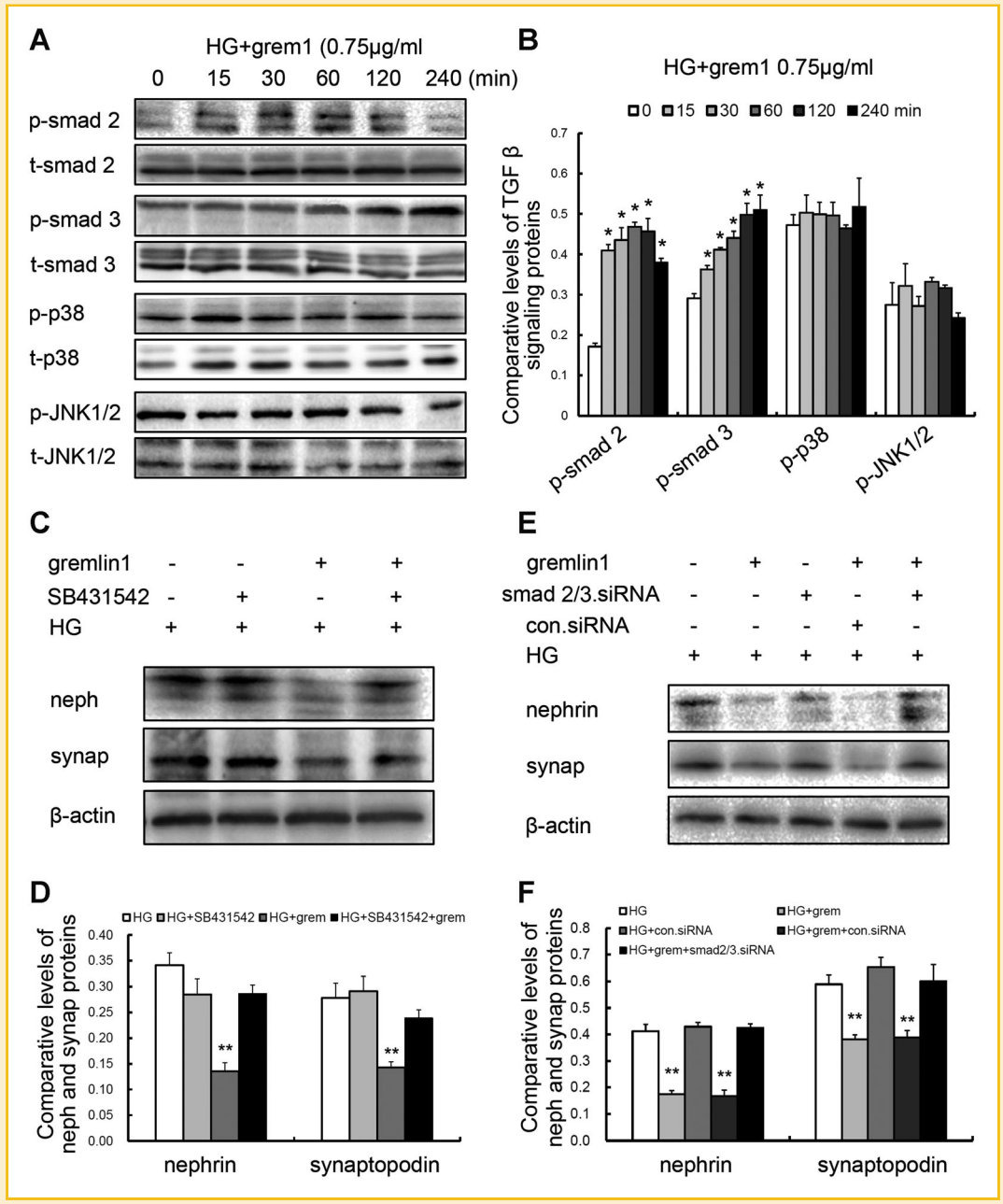

Fig. 7. The role of the TGF-β signaling pathway in gremlin and high glucose cultured podocytes. A: The protein of TGF-β signaling molecules (smad2/p-smad2, smad3/p-smad3, p38/p-p38, and JNK1/2/P-JNK1/2) was analyzed by Western blot. Gremlin activated the canonical but not the non-canonical signaling pathway in hyperglycemia podocytes. B: The protein level of TGF-β signaling molecules (smad2/p-smad2, smad3/p-smad3, p38/p-p38 and JNK1/2/P-JNK1/2) was quantified by densitometry. $^{*}P < 0.05$ versus controls (0 min). C,D: The TGF-β receptor inhibitor (SB431542) blocked the ability of gremlin to suppress the expression of nephrin and synaptopodin protein in podocytes. $^{**}P < 0.01$ versus SB431542 controls. E,F: Smad2/3 siRNA blocked the ability of gremlin to suppress expression of nephrin and synaptopodin in podocytes. β-Actin was used as a loading control. The values were expressed as means ± SD, n = 6. $^{**}P < 0.01$ versus smad2/3 siRNA controls.

DISCUSSION

In the present study, we found that the expression of gremlin was more significantly elevated in high-glucose cultured podocytes than in controls. The expression of gremlin was membrane-associated or displayed a scattered pattern of expression in the cytoplasm. This pattern of gremlin expression is concordant with its function. For example, expression of gremlin1 on renal cell membranes permits its binding of extracellular BMP-2 BMP-4, and BMP-7 and subsequent inhibition of smad-1, -5, and -8 signaling [Zhang and Zhang, 2009]. By contrast, expression of gremlin1 on the monocyte cell membrane allows binding of gremlin to the slit1 or slit2 receptor and to exert its

role [Dressler, 2009]. Thus, it is possible that many mechanisms remain to be identified in the context of gremlin and the regulation of cellular behavior [Wordinger et al., 2008]. Premature and mature gremlin expression is scattered in the cytoplasm where it binds intracellular BMPs and other unidentified molecules.

In vivo, gremlin1 regulates critical processes controlling limb-bud outgrowth and kidney development [Wang et al., 2001]. Knockout of the gremlin gene causes mice to die of postnatal renal aphasia. Gremlin is mainly expressed in podocytes and parietal epithelial cells in early diabetic glomerular nephropathy. It is also expressed at a relatively low level in the mesangial area in more advanced morphological lesions, but is absent in normal adult human kidney [Dolan et al., 2005; McMahon et al., 2000]. In advanced human diabetic nephropathy, gremlin expression is found to be abundant in tubule-interstitial fibrosis, and is co-localized with TGF-β1 [Michos et al., 2004]. These observations suggest that gremlin may have an important role in the onset and progression of DN. Of particular importance were the observations that the podocyte was injured in the early course of DN, and was seen a few years prior to the changes seen in GBM and the mesangial areas. These studies suggest that gremlin play an important role in podocytes injury in the early stage of DN. In vitro studies have provided evidence in support of the role played by gremlin in high-glucose cultured renal mesangial cells and tubular epithelial cells [Zhang et al., 2010; Sethi et al., 2011]. However, in vitro studies on the relationship between gremlin and podocyte are rare.

To mimic gremlin over-expression under conditions of ambient high glucose, podocytes were treated with recombinant mouse gremlin and D-glucose. We found that gremlin aggravated high glucose induced podocyte injury and further changed the distribution of nephrin and synaptopodin. In addition, we observed a time- and dose-dependent down-regulation of the protein and transcriptional expression of nephrin and synaptopodin by gremlin. Nephrin is located between intact adjacent of podocytes [Moeller and Holzman, 2006]. Synaptopodin is one of the major components of the podocyte cytoskeloton, which functions to modulate the morphology of the podocyte. Dysfunction of synptopodin acts to depolymerize the bundle of actin in the foot process, which is the executer of cellular mobility [Ichimura et al., 2003]. Both disturbed podocyte–GBM anchoring and podocyte–podocyte homotypic interactions at the level of glomerular epithelial slit diaphragms (GESDs) leads to the injury of podocytes, dysfunction of the glomerular filtration barrier, and ultimately, to glomerulosclerosis and renal failure [Kistler et al., 2012]. However, gremlin1 siRNA can rescue nephrin and synaptopodin expression and attenuate the altered morphology of podocytes cultured in high glucose. This observation suggests that gremlin serves a critical role in podocyte injury in DN.

Questions that interested us were whether gremlin could exerts its role via TGFβ/smad2/3 signaling in the context of TGF-β and BMP interactions, and whether subsequent smad2/3 signaling could play an important role in DN [Mitu et al., 2007]? Additionally, we wished to address the question of whether dampening the BMP/smad1/5/8 signaling pathway could activate TGFβ/smad2/3 signaling. To address these questions, we assessed the signaling pathway mediated by TGFβ/smad2/3 in gremlin treated podocytes. We found that gremlin exerted its effect on podocytes by activating a canonical smad2/3 signaling pathway, but did not activate a non-canonical JNK1/2 or MAPK signaling.

Inhibition of smad2/3 or TGF-β receptor signaling blocked the effects of gremlin on podocytes. It has been shown previously that binding of BMP by gremlin decreases smad1/5/8, which represents key markers of BMP signaling activation and does not reflect TGF-β signaling [Wang et al., 2006]. This notion does not contradict with observations made from our study. Perturbations in the balance of TGF/BMP signaling are associated with the development and severity of diabetic nephropathy. Gremlin protein levels are higher in high-glucose cultured podocytes, and gremlin blocks the ability of BMP to suppress TGF-β1-mediated effects on the podocyte.

TGF-β1 plays an important role in the pathogenesis of DN. The levels of TGF-β1 are significantly elevated not only in renal biopsy specimens derived from DN patients, but also elevated in various renal cells, including podocytes, mesangial cells and proximal tubular epithelial cells [Iglesias-de la Cruz et al., 2002; Li et al., 2012]. Podocytes express BMPs, BMP receptors and BMP antagonists [Pache et al., 2006]. Maintenance of renal BMP-7 during the evolution of DN reduces diabetic renal injury, especially podocyte dropout [Ichimura et al., 2003]. In our study, we found that TGF-β1 and gremlin induced each other's expression in podocytes. UP to now, it is unknown that how gremlin and TGF-β induce each other in diabetic nephropathy, though the phenomenon could be seen in renal cells and trabecular meshworkcell [Sethi et al., 2011] and some kinds of tumor cell lines [Pache et al., 2006]. In embryology, TGF-β, gremlin and FGF (fibroblast growth factor) regulate each other through a complex feedback loop [Benazet et al., 2009]. But if this regulation exists in diabetic nephropathy is unknown. These findings also establish that gremlin enhances TGF-β or promotes to weaken BMP signaling such that this results in the disruption of normal TGF-β1/BMP homeostasis. TGF-β/smad signaling activation various in context of different cell lines. In many cancer cell and fibroblast it needs 12 h or more for TGF-β to activate smad proteins [Pannu et al., 2007], but only need 15 min–3 h in renal podocyte, mesangial cell or proximal epithelial cell [Zhu et al., 2010]. When podocyte expose to high ambient glucose, TGF-β1 increase in few minutes and to a significant level in 2–3 h. This increasing is parallel with that of smad protein.

We suggest that gremlin injurys podocytes by disturbing the balance between BMP and TGF-β1. Gremlin binds to BMP and by doing so, inhibits the ability of BMP to modulate and induce podocyte motility in response to TGF-β1. We showed that prior to treating podocytes with gremlin, pretreatment with specific siRNA or small molecule inhibitors effectively quenched endogenous expression of TGF-β1. Under these circumstances, gremlin exerts no effect on the podocyte since there was no longer an endogenous TGF-β signaling pathway that would otherwise dampen the expression of nephrin and synaptopodin.

Most studies of gremlin have focused on its role in the development of fibrotic disease [Lappin et al., 2002]. It is quite common to find reemergence of developmental genes in idiopathic pulmonary fibrosis, cancer, and glaucoma. However, additional studies are needed to address this hypothesis in DN [Roxburgh et al., 2009]. It also appears that gremlin, TGF-β1 and connective tissue growth factor (CTGF) are involved in a "feed-forward" pathogenic pathway [Dolan et al., 2003].

We have shown that gremlin increases TGF-β1 expression, and that TGF-β1 increases gremlin expression in high-glucose cultured podocytes. This process would further exacerbate podocyte injury, potentially leading to more GBM nudy and glomerulosclerosis. Levels of TGF-β1 and gremlin are elevated in DN, yet the primary mechanisms responsible for the enhanced expression of these signaling molecule remains unknown. Others have shown that the cyclic mechanical strain and hyperglycemia increases TGF-β1 expression in DN [Weil et al., 2011]. The effects of these perturbations on gremlin expression have not yet been evaluated.

We first established that elevated gremlin leads to higher TGF-β1 levels in high-glucose cultured podocytes. Since TGF-β displays pleiotropic actions, it may not be an ideal therapeutic target [Li et al., 2006]. However, gremlin is a downstream mediator of TGF-β signaling, and may serve as a therapeutic target in the management of DN [Wada et al., 2002]. Our results indicate that siRNA-mediated targeting of gremlin1 rescues the expression of nephrin and synaptopodin in ambient hyperglycemic podocytes and suppresses their motility. The limitation of this study is that it is an in vitro observational approach, and of course, future work will focus more on in vivo mechanisms of action.

In summary, gremlin plays an important role in the pathogenesis of podocyte injury in DN, perhaps by disrupting the homeostatic balance between TGF-β and BMP. There also appears to be a feedback loop between gremlin and TGF-β1 whereby they are capable of inducing each other and accelerating the pathogenesis of the disease process. Gremlin activates a canonical smad2/3 pathway, but does not activate a non-canonical pathway of TGF-β signaling. New therapies targeting gremlin may protect the kidney from the development and progression of DN. With this in mind, further studies of gremlin as a therapeutic target in the treatment of DN are clearly warranted. Some important questions that remain unanswered include the following; (1) Does modulating mechanism of developmental gene expression in the embryo play a role in DN [Roxburgh et al., 2006]? (2) Does a feedback loop exist among sonic hedgehog (shh), gremlin and fibroblast growth factor (FGF) in DN, as has been reported in embryogenesis [Benazet et al., 2009]? (3) Dose a specific receptor exist that is capable of directly binding gremlin1 in podocytes [Wordinger et al., 2008]? (4) Do different gremlin signaling mechanisms regulate DN [Murphy et al., 2002]? Our present study provides a foundation to address these questions in future studies. The present work, then, has important implications for the future development of inhibitory strategies that could directly target gremlin.

ACKNOWLEDGMENTS

The authors thank Dr. Wei Liu for his expert assistance with this project. The assistance and advice of the staff at the Department of Pathology at the Hebei Medical University are also greatly appreciated.

REFERENCES

Babayeva S, Zilber Y, Torban E. 2011. Planar cell polarity pathway regulates actin rearrangement, cell shape, motility, and nephrin distribution in podocytes. Am J Physiol Renal Physiol 300:F549–F560.

Benazet JD, Bischofberger M, Tiecke E, Goncalves A, Martin JF, Zuniga A, Naef F, Zeller R. 2009. A self-regulatory system of interlinked signaling feedback loops controls mouse limb patterning. Science 323:1050–1053.

Diez-Sampedro A, Lenz O, Fornoni A. 2011. Podocytopathy in diabetes: A metabolic and endocrine disorder. Am J Kidney Dis 58:637–646.

Dolan V, Murphy M, Alarcon P, Brady HR, Hensey C. 2003. Gremlin—A putative pathogenic player in progressive renal disease. Expert Opin Ther Targets 7:523–526.

Dolan V, Murphy M, Sadlier D, Lappin D, Doran P, Godson C, Martin F, O′Meara Y, Schmid H, Henger A, Kretzler M, Droguett A, Mezzano S, Brady HR. 2005. Expression of gremlin, a bone morphogenetic protein antagonist, in human diabetic nephropathy. Am J Kidney Dis 45:1034–1039.

Dressler GR. 2009. Advances in early kidney specification, development and patterning. Development 136:3863–3874.

Faul C, Donnelly M, Merscher-Gomez S, Chang YH, Franz S, Delfgaauw J, Chang JM, Choi HY, Campbell KN, Kim K, Reiser J, Mundel P. 2008. The actin cytoskeleton of kidney podocytes is a direct target of the antiproteinuric effect of cyclosporine A. Nat Med 14:931–938.

Ichimura K, Kurihara H, Sakai T. 2003. Actin filament organization of foot processes in rat podocytes. J Histochem Cytochem 51:1589–1600.

Iglesias-de la Cruz MC, Ziyadeh FN, Isono M, Kouahou M, Han DC, Kalluri R, Mundel P, Chen S. 2002. Effects of high glucose and TGF-beta1 on the expression of collagen IV and vascular endothelial growth factor in mouse podocytes. Kidney Int 62:901–913.

Jefferson JA, Alpers CE, Shankland SJ. 2011. Podocyte biology for the bedside. Am J Kidney Dis 58:835–845.

Kistler AD, Altintas MM, Reiser J. 2012. Podocyte GTPases regulate kidney filter dynamics. Kidney Int 81:1053–1055.

Lappin DW, Hensey C, McMahon R, Godson C, Brady HR. 2000. Gremlins, glomeruli and diabetic nephropathy. Curr Opin Nephrol Hypertens 9:469–472.

Lappin DW, McMahon R, Murphy M, Brady HR. 2002. Gremlin: An example of the re-emergence of developmental programmes in diabetic nephropathy. Nephrol Dial Transplant 17(Suppl9):65–67.

Li MO, Wan YY, Sanjabi S, Robertson AK, Flavell RA. 2006. Transforming growth factor-beta regulation of immune responses. Annu Rev Immunol 24:99–146.

Li W, Cui M, Wei Y, Kong X, Tang L, Xu D. 2012. Inhibition of the expression of TGF-beta1 and CTGF in human mesangial cells by exendin-4, a glucagon-like peptide-1 receptor agonist. Cell Physiol Biochem 30:749–757.

McMahon R, Murphy M, Clarkson M, Taal M, Mackenzie HS, Godson C, Martin F, Brady HR. 2000. IHG-2, a mesangial cell gene induced by high glucose, is human gremlin. Regulation by extracellular glucose concentration, cyclic mechanical strain, and transforming growth factor-beta1. J Biol Chem 275:9901–9904.

Michos O, Panman L, Vintersten K, Beier K, Zeller R, Zuniga A. 2004. Gremlin-mediated BMP antagonism induces the epithelial–mesenchymal feedback signaling controlling metanephric kidney and limb organogenesis. Development 131:3401–3410.

Mitu GM, Wang S, Hirschberg R. 2007. BMP7 is a podocyte survival factor and rescues podocytes from diabetic injury. Am J Physiol Renal Physiol 293: F1641–F1648.

Moeller MJ, Holzman LB. 2006. Imaging podocyte dynamics. Nephron Exp Nephrol 103:e69–e74.

Murphy M, McMahon R, Lappin DW, Brady HR. 2002. Gremlins: Is this what renal fibrogenesis has come to? Exp Nephrol 10:241–244.

Murphy M, Crean J, Brazil DP, Sadlier D, Martin F, Godson C. 2008. Regulation and consequences of differential gene expression in diabetic kidney disease. Biochem Soc Trans 36:941–945.

Pache G, Schafer C, Wiesemann S, Springer E, Liebau M, Reinhardt HC, August C, Pavenstadt H, Bek MJ. 2006. Upregulation of Id-1 via BMP-2 receptors induces reactive oxygen species in podocytes. Am J Physiol Renal Physiol 291: F654–F662.

Pannu J, Nakerakanti S, Smith E, Dijke PT, Trojanowska M. 2007. Transforming growth factor-β receptor type I-dependent fibrogenic gene program is mediated via activation of smad1 and ERK1/2 pathways. J Biol Chem 282:10405–10413.

Roxburgh SA, Murphy M, Pollock CA, Brazil DP. 2006. Recapitulation of embryological programmes in renal fibrosis—The importance of epithelial cell plasticity and developmental genes. Nephron Physiol 103:39–148.

Roxburgh SA, Kattla JJ, Curran SP, O′Meara YM, Pollock CA, Goldschmeding R, Godson C, Martin F, Brazil DP. 2009. Allelic depletion of grem1 attenuates diabetic kidney disease. Diabetes 58:1641–1650.

Sethi A, Jain A, Zode GS, Wordinger RJ, Clark AF. 2011. Role of TGFbeta/Smad signaling in gremlin induction of human trabecular meshwork extracellular matrix proteins. Invest Ophthalmol Vis Sci 52:5251–5259.

Smerdel-Ramoya A, Zanotti S, Canalis E. 2011. Nephroblastoma over-expressed (Nov) induces gremlin in ST-2 stromal cell lines by post-transcriptional mechanisms. J Cell Biochem 112:715–722.

Wada J, Makino H, Kanwar YS. 2002. Gene expression and identification of gene therapy targets in diabetic nephropathy. Kidney Int 61:S73–S78.

Wada J, Sun L, Kanwar YS. 2011. Discovery of genes related to diabetic nephropathy in various animal models by current techniques. Contrib Nephrol 169:161–174.

Wang SN, Lapage J, Hirschberg R. 2001. Loss of tubular bone morphogenetic protein-7 in diabetic nephropathy. J Am Soc Nephrol 12:2392–2399.

Wang S, de Caestecker M, Kopp J, Mitu G, Lapage J, Hirschberg R. 2006. Renal bone morphogenetic protein-7 protects against diabetic nephropathy. J Am Soc Nephrol 17:2504–2512.

Weil EJ, Lemley KV, Yee B, Lovato T, Richardson M, Myers BD, Nelson RG. 2011. Podocyte detachment in type 2 diabetic nephropathy. Am J Nephrol 33 (Suppl1):21–24.

Wordinger RJ, Zode G, Clark AF. 2008. Focus on molecules: Gremlin. Exp Eye Res 87:78.

Zhang Y, Zhang Q. 2009. Bone morphogenetic protein-7 and Gremlin: New emerging therapeutic targets for diabetic nephropathy. Biochem Biophys Res Commun 383:1–13.

Zhang Q, Shi Y, Wada J, Malakauskas SM, Liu M, Ren Y, Du C, Duan H, Li Y, Zhang Y. 2010. In vivo delivery of Gremlin siRNA plasmid reveals therapeutic potential against diabetic nephropathy by recovering bone morphogenetic protein-7. PLoS ONE 5:e 11709.

Zhu B, Wang YJ, Zhu CF, Lin Y, Zhu XL, Wei S, Lu Y, Cheng XX. 2010. Triptolide inhibits extracellular matrix protein synthesis by suppressing the smad2 but not the MAKP pathway in TGF-β1-stimulated NRK-49F cells. Nephrol Dial Transplant 25:3180–3191.